JTTEE5 11:530-535

Corrosion of Thermal Spray Hastelloy C-22 Coatings in Dilute HCl

T.E. Lister, R.N. Wright, P.J. Pinhero, and W.D. Swank

(Submitted 28 February 2001; in revised form 5 June 2001)

The microstructure and corrosion behavior of Hastelloy C-22 coatings produced using the high velocity oxygen fuel (HVOF) method have been determined and related to in-flight measurements of the particle velocity and temperature. Average particle temperatures ranged from 1280-1450 °C and velocities ranged from 565-640 ms^{-1}. All of the coatings were greater than 98% of theoretical density and exhibited passivating behavior in 0.1 M HCl during cyclic potentiodynamic polarization testing. The passive current density was somewhat higher compared with wrought C-22 alloy and an active-passive peak attributed to the formation of a Cr-rich surface layer was observed. Resistance to corrosion and deposition efficiency improved as the particle temperature decreased. There was little effect of particle velocity on the corrosion behavior over the range of deposition conditions examined. Our results suggest that feedback control based on measurement of the particle temperature can be used to process coatings with optimum properties.

Keywords corrosion, Hastelloy, high velocity oxygen fuel (HVOF) process, polarization behavior

1. Introduction

Many thermal spray processes and materials systems have been investigated to produce corrosion-resistant coatings on metallic substrates. Relatively low cost and low melting point coatings of aluminum or zinc have been investigated for protection or refurbishment of large civil engineering structures. Many of these coatings have been produced with processes that result in substantial porosity and depend on the intrinsic cathodic protection afforded by the coating chemistry, or the coatings are subsequently impregnated with polymers to seal porosity.[1] Coatings containing hard phases for improving wear and erosion resistance, in addition to improving corrosion behavior, have also been developed.[2-4] The latter alloys are frequently based on Ni-Cr-W-Mo composition with a metalloid element such as boron added to promote formation of hard amorphous phases.

Near full density metallic coatings of conventional corrosion resistant stainless steel and nickel based alloy compositions have been deposited using plasma spray or high velocity oxygen fuel (HVOF) processes.[5-9] In cases for which direct comparison of plasma spray and HVOF methods has been made, the corrosion resistance of the HVOF coatings has been superior.[5,10] Corrosion performance of coatings has been related to the processing parameters that are available for experimental control; for example, the power input for plasma spray or the fuel-to-oxygen ratio for HVOF. Electrochemical methods have also been used to characterize the influence of processing parameters on microstructure features and their relationship to the corrosion behavior.[8,9] In general, the corrosion resistance is improved by reducing porosity and oxide content. It has also been reported that the resistance to corrosion is improved by reducing the fraction of unmelted particles in the coating.[7,9] Boundaries between splats that make up the coating have been found to be particularly susceptible to corrosion because of the presence of oxides or because volatilization of alloy constituents has changed the local chemistry.[3,11,12]

HVOF is a combustion process that uses oxygen and a liquid or gaseous fuel such as propylene or kerosene to heat and accelerate powder feedstock that is fed into the flame. In a typical HVOF process, metallic particles are deposited near or below their melting temperature and have velocity at impact of approximately 500-700 ms^{-1}.[13,14] In contrast, plasma spray processes heat metallic particles well into the molten condition and particle velocities of 100-200 ms^{-1} are more usual.

A range of austenitic stainless steels and high Cr nickel alloys have been examined for corrosion resistance in geological disposal of spent nuclear fuel and high-level nuclear waste.[15-19] Hastelloy C-22 (UNS N06022, Haynes International, Inc., Kokomo, IN) is one of the primary candidate container materials for long-term storage in the United States.[19] Although the alloy in wrought form is likely to be used for structural purposes, stainless steel or C-22 alloy thermal spray coatings containing Gd oxide as a neutron poison material are under consideration for application to structures on the inside of the storage cask. This study examined the influence of processing conditions on the microstructure and electrochemical corrosion behavior of HVOF sprayed C-22 alloy in HCl solution. In-flight measurements were made of the average particle temperature and velocity, and the microstructure and corrosion behavior is related to the measured particle characteristics. In this way, the results should be generally applicable rather than specific to particular process parameters with one type of HVOF gun. Presumably, any system capable of depositing particles with the same temperature and velocity will produce coatings with similar corrosion behavior.

T.E. Lister, R.N. Wright, P.J. Pinhero, and **W.D. Swank,** Idaho National Engineering and Environmental Laboratory, P.O. Box 1625, Idaho Falls, ID 83415-2218. Contact e-mail: RNWZ@inel.gov.

2. Experimental Procedure

Coatings were deposited using a TAFFA JP-5000 HVOF torch (Concord, NH). This torch operates with liquid kerosene fuel and oxygen. Nearly spherical gas-atomized C-22 alloy powder from Anval, Inc. (Rutherford, NJ) with a particle size range of 16-44 μm was used in all of the experiments. The composition of the starting C-22 alloy powder is given in Table 1. Coatings were produced on grit-blasted type 316L substrates in laboratory air without any additional shielding gas. They were built up in layers by rastering the substrate in the particle plume from a fixed-position torch. A transverse velocity of 200 mm s^{-1} and standoff distance of 355 mm was used for deposition of all of the coatings. Substrates were air cooled from behind during coating.

The HVOF system used in these experiments can operate over a wide range of fuel-oxygen mixtures and combustion chamber pressures. It has been shown previously that the fuel-oxygen ratio and the chamber pressure independently control the combustion gas temperature and dynamic pressure available to heat and accelerate the particles, respectively.[13] In the current experiments the fuel-to-oxygen ratio and the chamber pressure were varied in an effort to independently vary the particle velocity and temperature. A fixed barrel length of 200 mm was used for all of the coatings.

Particle velocity was measured using a modified Aerometrics Phase Doppler Anemometer (Sunnyvale, CA) system.[20] The velocity of approximately 2000 particles was measured on the centerline of the spray and averaged for each torch operating condition. The measurement volume of an Inflight Particle Pyrometer (Inflight Ltd., Idaho Falls, ID) was directed coincident with that of the phase Doppler anemometer to simultaneously measure the average particle temperature.[21] All measurements were made at the substrate standoff distance of 355 mm. Uncertainty in particle temperature and velocity measurements is on the order of 5%.

Microstructures were characterized using optical and scanning electron microscopy (SEM). Optical images from cross sections through the coating were examined in the as-polished condition to determine the area fraction of porosity. Polished cross sections were electrolytically etched using 10% oxalic acid in water to reveal the solidification structure in the powder prior to measuring the area fraction of unmelted particles. Oxide fraction was measured from backscattered electron (SEM) images and the values were corrected for the area fraction of porosity measured optically. Measurements were made using standard point counting methods from four different areas on each coating, with a total of 1000 points counted.

Corrosion testing was performed using potentiodynamic methods based on the American Society for Testing and Materials (ASTM) G5 procedure. The corrosion medium was 0.1 M hydrochloric acid made from American Chemical Society grade hydrochloric acid and water obtained from a four-stage filtration purification system. This solution was chosen as representative of the most aggressive water chemistry likely in the repository environment and was not aerated during testing. Samples were degreased with sequential increases in acetone, ethanol, and nanopure (Barnstead, Dubuque, IA) water before analysis. Gravimetric measurements were performed before and after corrosion testing using a five-place analytical balance. A Princeton Applied Research Corp. (Oak Ridge, TN) corrosion testing system was used, which included a model 263A potentiostat-galvanostat and model M270 software for computer controlled acquisition. A standard corrosion cell was used and samples were held in a flat specimen holder such that the surface of interest was exposed to the solution to an area of approximately 1.0 cm^2. Potentiodynamic scans were performed in a cyclic manner from −0.5-1.0 V versus a saturated calomel electrode (SCE) reference electrode at a sweep rate of 0.6 V hr^{-1}. Two scans over this range were performed for each sample except in cases noted below.

Table 1 Composition of the Gas Atomized Alloy C-22 Powder Used in These Experiments in wt.%

Ni	Mo	Cr	W	Fe	C	N	Si	P	S
56.7	13.7	21.1	3.02	5.15	0.023	0.091	0.54	0.015	0.008

Table 2 Measured In-Flight Particle Temperatures and Velocities for Different Equivalence Ratios and Gas Chamber Pressures (a)

Chamber Pressure, KPa	Equivalence Ratio	Average Particle Velocity, ms^{-1}	Average Particle Temperature, °C	Coating Thickness, μm
430	0.8	565	1280	565
610	0.6	604	1200	457
610	0.8	641	1365	424
610	1.0	635	1450	380
780	0.8	643	1415	320

(a) The coating thickness is a relative measure of deposition efficiency.

3. Results

The average particle velocity and temperature for the five different spray conditions at the substrate location are given in Table 2. Equivalence ratios listed in Table 2 are the fuel-to-oxygen ratio with respect to a stoichiometric mixture. An equivalence ratio of 1.0 represents stoichiometric combustion and the lower values represent an excess of oxygen. The particular values used here were selected to result in relatively low particle temperatures on the basis of previous characterization of the HVOF torch.[13] C-22 alloy has a melting point of approximately 1375 °C, thus for several coatings the average particle would be deposited below the melting point. For conditions where the average temperature is above 1400 °C, it is expected that some fraction of the particles, particularly smaller diameter particles, would be fully molten.

The particle velocity distribution was approximately Gaussian about the average, with a range of approximately 50 ms^{-1} on either side of the mean, except for the 0.6 equivalence ratio experiment that had two peaks in the distribution separated by approximately 100 ms^{-1}. The reason for this behavior is not clear; however, the result is that the range of velocities was about a total of 200 ms^{-1}. Table 2 also includes measurement of the coating thickness. Because all of the coatings were processed with identical powder feed conditions, traverse velocity, and number of passes, the thickness can be taken as a relative measure of the deposition efficiency.

All of the coatings were free of cracks and well bonded to the substrate. The area fraction of porosity and unmelted particles were measured from optical micrographs of cross-sections through the coatings (Table 3). Representative examples of etched cross sections for coatings formed from particles with low and high average temperature are shown in Fig. 1(a) and (b), respectively. The dendritic solidification structure is clearly visible in the unmelted particles; these particles have a characteristic shape resulting from the high-velocity impact with the substrate. Unmelted particles deposited at higher velocity were more flattened compared with the nearly hemispherical shape shown in Fig. 1(a) for relatively low temperature and low velocity particles. The area fraction of porosity is low for all of the spray conditions examined and there is no clear correlation with particle temperature or velocity. Porosity is often associated with unmelted particles; however, there is no consistent correlation with the fraction of unmelted particles for the coatings examined here.

The area fraction of oxide, measured from backscattered electron images and corrected for porosity, is included in Table 3. Representative backscattered electron micrographs are shown in Fig. 2(a) and (b) for coatings deposited with average particle temperatures of 1280 and 1450 °C, respectively. It is evident from the values given in Table 3 that the area fraction of oxide increases as the particle temperature increases. The particle velocity does not appreciably affect the fraction of oxide, even though an influence caused differences in the residence time at elevated temperature might be expected.

Cyclic potentiodynamic polarization curves were measured for all of the coatings in the as-deposited condition. Representative curves for the coating deposited with particle temperature 1365 °C and velocity of 641 ms^{-1}, and for polished wrought C-22 alloy are shown in Fig. 3. All of the coating curves were qualitatively similar, showing passive behavior with increasing potential after a significant active-passive transition peak. The current density in the passive region generally increased somewhat with increasing particle temperature. For example, the coating deposited with average particle temperature of 1200 °C had a current density of 60 μAcm^{-2} at a potential of 800 mV compared with a value of 80 μAcm^{-2} for the coating deposited with particle temperature of 1450 °C. The wrought material exhibited a small active-passive transition peak at a potential similar to that observed for the coatings and had a current density in the passive region of less than 1 μAcm^{-2}. Electrochemical data for all of the coatings are shown in Table 4. For samples cycled to potentials into the transpassive region, greater than about 800 mV, measurable weight loss was observed and chemical analysis of the test solution indicated that the weight loss was primarily the result of dissolution of Ni.

4. Discussion

As noted above, polarization curves for the coatings differed from the wrought alloy in several significant respects. Polarization curves in Fig. 3 that compare as-sprayed coating material to a polished wrought alloy indicate higher current density in the passive region. Higher current density might be a reflection of the greater surface area of the coating resulting from the rough surface that is typical of thermal spray coatings. To examine this issue, a coating polished through 0.25 μm diamond was tested under conditions identical to those used to obtain the coating curve shown in Fig. 3, and resulted in the current density being reduced by a factor of two. Thus, some portion of the difference in corrosion behavior is attributable to the rough surface of the as-sprayed coatings, but there remains an intrinsic difference in the material properties.

Table 3 Microstructural Characteristics Associated With Particle Velocity and Temperature

Average Particle Velocity, m/s	Average Particle Temperature, °C	Area Fraction of Porosity, %	Fraction of Unmelted Particles, %	Area Fraction of Oxide, %
565	1280	2.1	36	9.1
604	1200	0.8	26	4.2
641	1365	1.5	2.2	13.7
635	1450	0.7	4.7	16.3
643	1415	1.2	4.0	16.3

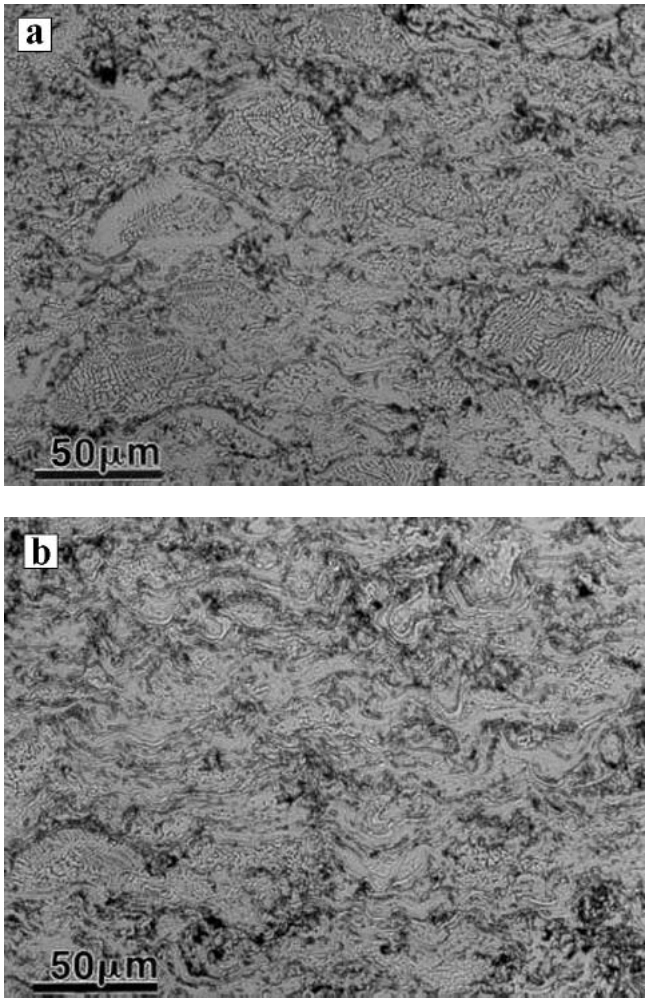

Fig. 1 Optical micrographs of etched cross-sections through coatings deposited with average particle temperature and velocity of **(a)** 1280 °C and 565 m/s and **(b)** 1450 °C and 635 m/s. The fine dendritic solidification microstructure resulting from the gas atomization is evident in the unmelted particles.

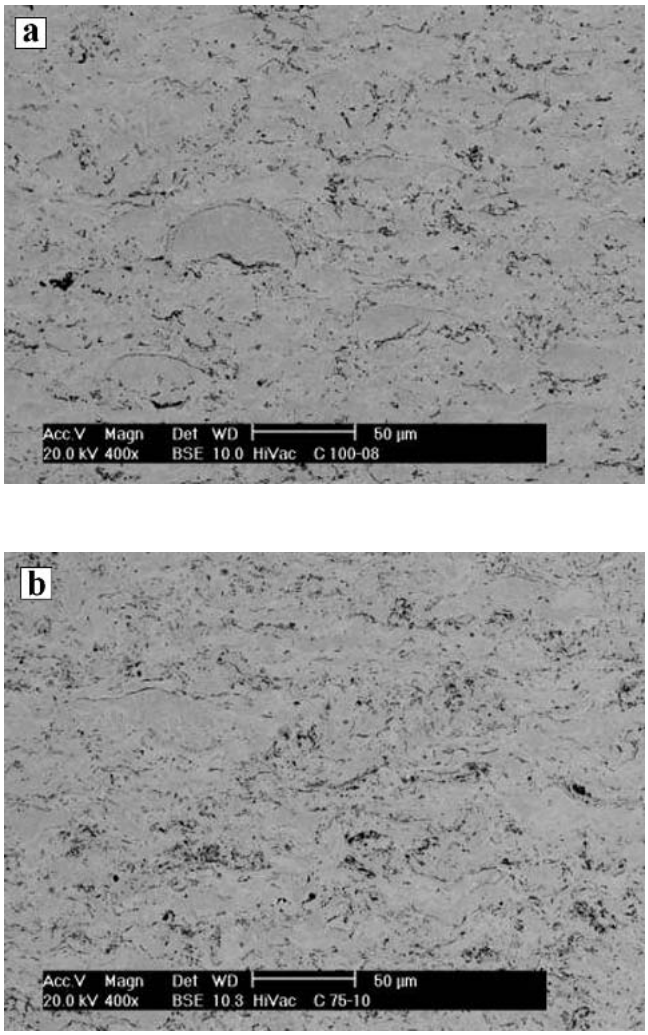

Fig. 2 Backscattered electron micrographs of C-22 coatings deposited with average particle temperatures of **(a)** 1280 and **(b)** 1450 °C

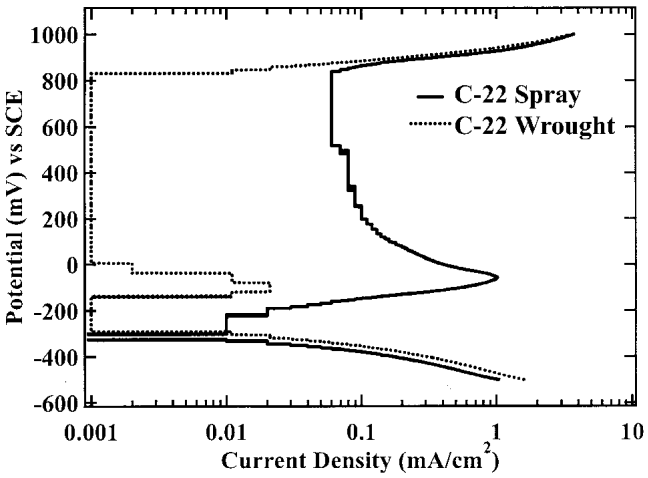

Fig. 3 Polarization curves for as-deposited C-22 alloy coating deposited with a particle temperature of 1365 °C and velocity of 641 ms^{-1} and a polished specimen of wrought C-22 alloy

Table 4 Electrochemical Properties of C-22 Alloy Coatings

Average Particle Velocity, m/s	Average Particle Temperature, °C	Charge Associated With Prepassivation Peak, C	Current in Passive Region, mA
565	1280	0.04	0.12
604	1200	0.20	0.06
641	1365	0.65	0.06
635	1450	0.78	0.08
643	1415	0.79	0.1

All of the coating materials tested exhibited a substantial active-passive peak. The total current associated with the active-passive peak, obtained from the integrated area under the peak in the polarization plots, is shown as a function of the particle temperature in Fig. 4. The magnitude of the peak increases as the particle temperature increases. The presence of an active-passive peak in the polarization curve has also been reported for both wrought and thermal spray coating Ni-Cr alloys under some conditions of pH and chloride concentration.[9,16,17] Although the exact mechanism of the passivation reaction is not yet known, it appears that C-22 alloy coatings deposited with higher temperature particles have a surface chemistry different from wrought material and coatings deposited at lower temperature, and greater alteration of the surface is necessary for passivation to occur. If the coating is cycled twice though the potential range shown in Fig. 3, both the magnitude of the active-passive peak and the current density in the passive region are reduced after the first scan. A typical pair of scans is shown in Fig. 5. This suggests that the surface layer that is formed is passivating and will protect the coating from further corrosion.

For the conditions examined here, the lowest particle temperature resulted in the highest relative deposition efficiency. It has been shown previously through careful examination of splats collected on polished substrates that fully molten particles tend to fragment on impact and smaller fragments rebound rather than becoming incorporated into the coating.[22] Higher velocity was found to result in greater fragmentation and lower deposition efficiency.[22] Many investigators have shown that corrosion resistance is improved as the porosity decreases, which might be expected to favor deposition at higher velocity. Apparently, for C-22 alloy, particle velocities of greater than 500 ms^{-1} are sufficient to produce coatings with high enough density to provide corrosion protection even for particle temperatures well below the nominal melting point.

In another study, it was reported that corrosion performance of thermal spray nickel based coatings improved as the fraction of unmelted particles declined.[9] However, careful examination of those results suggests that it was the porosity associated with the unmelted particles, rather than the unmelted particles themselves, that caused increased corrosion as the unmelted fraction increased. Microstructural characterization of C-22 alloy coatings that were polished before cyclic polarization up to a potential of 1 V, where weight loss was shown to occur, indicated that material removal occurred in the regions between splats and adjacent to unmelted particles. An SEM micrograph is shown in Fig. 6 from the coating deposited with a particle temperature of 1365 °C and velocity of 641 ms^{-1} that was polished prior to

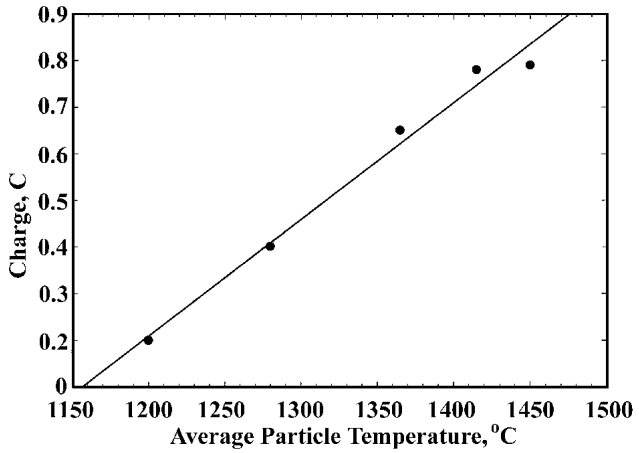

Fig. 4 Total charge associated with the active-passive peak as a function of average particle temperature. A linear regression line is included in the figure.

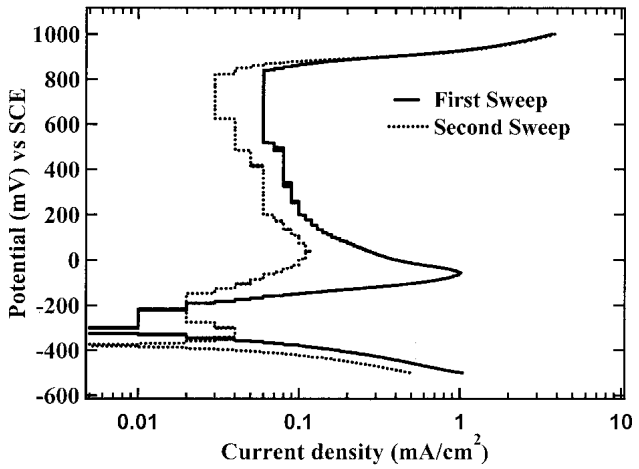

Fig. 5 Repeated polarization curves for the coating deposited with particle temperature of 1365 °C and velocity of 641 ms^{-1}. The second cycle results in a smaller active-passive peak and reduced current density in the passive region.

testing. An unmelted particle is apparent in the micrograph from the characteristic dendritic solidification structure resulting from gas atomization. It is evident from the micrograph that material removal occurred in the region surrounding the unmelted particle rather than from the unmelted particles.

It was noted above that measurable weight loss occurred with loss of Ni from the alloy if the polarization potential was increased into the transpassive region (above about 800 mV) and the amount of weight loss generally was found to increase with increasing particle temperature. It has been shown for Inconel 625 that the thermal spray process results in the formation of Cr_2O_3 as the major surface oxide interspersed with Ni of low alloy content.[12] This study on Inconel 625 reported that significant particle oxidation occurred with spray conditions that were fuel rich, presumably as a result of air entrained into the plume downstream from the torch.[12] For the oxidizing conditions examined in this study, higher particle temperature results in

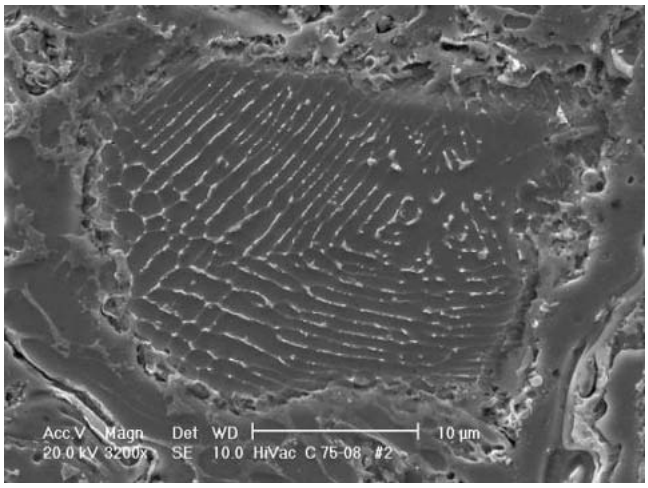

Fig. 6 Secondary electron micrograph of a polished C-22 alloy coating after cyclic polarization taken to a potential into the transpassive region. The area in the center of the micrograph exhibits the characteristic dendritic solidification structure resulting from gas atomization.

greater oxidation and should result in a corresponding increase in the amount of low alloy Ni. It is likely that dissolution of this low alloy Ni phase is responsible for increasing weight loss for coatings deposited from higher temperature particles. This is consistent with the observation that material removal occurred from regions that were fully molten prior to impact.

There has been recent progress in developing feedback control for thermal spray on the basis of real-time measurement of the average particle temperature.[23] It is fortuitous that both the deposition efficiency and several measures of the corrosion performance for C-22 alloy coatings are improved with the minimum particle temperature examined here. This work demonstrates that for HVOF deposition of this material, the particle temperature is a useful measure for on-line coating quality control rather than the more traditional postmortem electrochemical or microstructure characterization.

5. Conclusions

High-density, well-bonded coatings of C-22 alloy were deposited on stainless steel coupons using an HVOF torch. By varying the kerosene-to-oxygen stoichiometry and the chamber pressure, particle temperatures were varied from approximately 1200-1450 °C, and velocities varied from 565-640 ms^{-1}. Coatings deposited with the lowest particle temperature had approximately 2% porosity and 36% unmelted particles in the coating, whereas those processed at the highest temperature had 0.7% porosity and 4.7% unmelted particles.

Potentiodynamic polarization experiments showed that all of the coatings exhibited passivating behavior, but with higher current density in the passive region compared with wrought C-22 alloy. Increased current was in part an effect of higher surface area associated with surface roughness in the thermal spray coatings; the current was reduced by a factor of two by polishing the coating prior to testing. The current density in the passive region increased as the temperature of the particles used to form the coating increased.

The coatings also exhibited a notable active-passive peak that is associated with formation of a Cr-rich surface on the coating. The magnitude of the current associated with the active-passive peak increased as the particle temperature increased. Particle velocity was found to have little influence on the corrosion performance of the coatings. These results suggest that process control on the basis of the in-flight particle temperature could be used to ensure corrosion performance.

Acknowledgment

This work was supported by the United States Department of Energy, Assistant Secretary for Environmental Management, under DOE Idaho Operations Office Contract DE-AC07-99ID13727.

References

1. S. Tobe: "A Review on Protection From Corrosion, Oxidation, and Hot Corrosion by Thermal Spray Coatings" in *Thermal Spray: Meeting the Challenges of the 21st Century,* C. Coddet, ed., ASM International, Materials Park, OH, 1998, pp. 3-11.
2. T. Valente: "Air Plasma Sprayed Metallic Coatings for Sour Environments," *Br. Corr. J*., 2000, *35*(3), pp. 189-94.
3. A.H. Dent, A.J. Horlock, D.G. McCartney, and S.J. Harris: "The Corrosion Behavior and Microstructure of High-Velocity Oxy-Fuel Sprayed Nickel-Base Amorphous/Nanocrystalline Coatings," *J. Therm. Spray Technol*., 1999, *8*(3), pp. 399-404.
4. S. Sampath, R.A. Neiser, H. Herman, J.P. Kirkland, and W.T. Elam: "A Structural Investigation of a Plasma Sprayed Ni-Cr Based Alloy Coating," *J. Mater. Res*., 1993, *8*(1), pp. 78-86.
5. R. Hofman, M.P.W. Vreijling, G.M. Ferrari, and J.H.W. de Wit: "Electrochemical Methods for Characterization of Thermal Spray Corrosion Resistant Stainless Steel Coatings," *Mater. Sci. Forum*, 1998, *289-292,* pp. 641-54.
6. A.J. Sturgeon and D.C. Buxton: "The Electrochemical Corrosion Behavior of HVOF Sprayed Coatings" in *Thermal Spray: Surface Engineering Via Applied Research*, C.C. Berndt, ed., ASM International, Materials Park, OH, 2000, pp. 1011-15.
7. B. Normand, B. Laio, O. Landemarre, C. Coddet, and J. Pagetti: "Corrosion Resistance of Thermal Spray Inconel 690 Coatings" in *Thermal Spray: Meeting the Challenges of the 21st Century,* C. Coddet, ed., ASM International, Materials Park, OH, 1998, pp. 69-73.
8. M.P.W. Vreijling, R. Hofman, E.P.M van Westing, G.M. Ferrari, and J.H.W. deWit: "The Use of Electrochemical Techniques Towards Quality Control and Optimization of Corrosion Properties of Thermal Spray Coatings," *Mater. Sci. Forum*, 1998, *289-292,* pp. 595-606.
9. B. Normand, W. Herbin, O. Landemarre, C. Coddet, and J. Pagetti: "Electrochemical Methods to the Evaluation of Thermal Spray Coatings Corrosion Resistance," *Mater. Sci. Forum*, 1998, *289-292,* pp. 607-12.
10. M. Dvorak and P. Heimgartner: "Assessment of HVOF Coatings for Wet Corrosion Protection" in *Thermal Spray: Meeting the Challenges of the 21st Century,* C. Coddet, ed., ASM International, Materials Park, OH, 1998, pp. 95-100.
11. D. Harvey, O. Lunder, and R. Henriksen: "The Development of Corrosion Resistant Coatings by HVOF Spraying" in *Thermal Spray: Surface Engineering Via Applied Research*, C.C. Berndt, ed., ASM International, Materials Park, OH, 2000, pp. 991-97.
12. H. Edris, D.G. McCartney, and A.J. Sturgeon: "Microstructural Characterization of HVOF Sprayed Coatings of Inconel 625," *J. Mater. Sci*., 1997, *32,* pp. 863-72.
13. R.N. Wright, J.R. Fincke, W.D. Swank, D.C. Haggard, and C.R. Clark: "The Influence of Process Parameters on the Microstructure and Properties of Fe_3Al Based Coatings" in *Elevated Temperature Coatings: Science and Technology I,* N.B. Dahortre, J.M. Hampikian, and J.J. Stiglich, ed., TMS, Warrendale, PA, 1995, pp. 157-66.
14. W.D. Swank, J.R. Fincke, D.C. Haggard, G. Irons, and R. Bullock: "HVOF Particle Flow Field Characteristics" in *Thermal Spray Industrial Applications*, C.C. Berndt and S. Sampath, ed., ASM International, Materials Park, OH, 1994, pp. 319-24.
15. D. Druyts, B. Kursten, and P. Van Iseghem: "Electrochemical Study of the Pitting Corrosion of Stainless Steel Candidate Overpack Materials for the Disposal of High-Level Radioactive Waste in Boom Clay," *Mater. Sci. Forum*, 1998, *289-292,* pp. 1083-90.
16. N. Sridhar and G.A. Cragnolino: "Applicability of Repassivation Potential for Long-Term Prediction of Localized Corrosion of Alloy 825 and Type 316L Stainless Steel," *Corrosion*, 1993, *49*(11), pp. 885-94.
17. G.A. Cragnolino and N. Sridhar: "Localized Corrosion of a Candidate Container Material for High-Level Nuclear Waste Disposal," *Corrosion*, 1991, *47*(6), pp. 464-72.
18. K.A. Gruss, G.A. Cragnolino, D.S. Dunn, and N. Sridhar: "Repassivation Potential for Localized Corrosion of Alloy 625 and C-22 in Simulated Repository Environments" in *Corrosion 98*, National Association of Corrosion Engineers, Houston, TX, 1998, pp. 149/1-149/15.
19. R.D. McCright and W.L. Clarke: "Waste Package Design and Container Materials Evaluation for the Yucca Mountain Repository" in *Corrosion 98*, National Association of Corrosion Engineers, Houston, TX, 1998, pp. 159/1-159/15.
20. J.R. Fincke, W.D. Swank, C.L. Jeffery, and C.A. Mancuso: "A Technique for the Simultaneous Measurement of Particle Size, Velocity and Temperature, Measurement Science and Technology," *Meas. Sci. Technol.*, 1999, *4,* p. 559.
21. W.D. Swank, J.R. Fincke, and D.C. Haggard: "A Particle Temperature Sensor for Monitoring and Control of the Plasma Spray Process" in *Advances in Thermal Spray Science and Technology*, C. Berndt and S. Sampath, ed., ASM International, Materials Park, OH, 1995, pp. 111-16.
22. R.N. Wright, J.R. Fincke, W.D. Swank, and D.C. Haggard: "Particle Velocity and Temperature Influences on the Microstructure of Plasma Sprayed Nickel" in *Thermal Spray: Practical Solutions for Engineering Problems*, C.C. Berndt, ed., ASM International, Materials Park, OH, 1996, pp. 511-16.
23. J.R. Fincke, W.D. Swank, D.C. Haggard, and T.M. Demney: "Feedback Control of the Subsonic Plasma Spray Process" in *Advances in Thermal Spray Science and Technology*, C. Berndt and S. Sampath, ed., ASM International, Materials Park, OH, 1995, pp. 117-22.